Two-photon absorption reveals low-energy excited states of a 2,5,8-triamino-heptazine chromophore

Charles W. Stark, Johanna Arak, Aleksander Trummal, Merle Uudsemaa, Meelis Sildoja, Jüri Pahapill, Alexander Rebane

Two-photon absorption reveals low-energy excited states of a 2,5,8-triamino-heptazine chromophore

Charles W. Stark*[a], Johanna Arak[a], Aleksander Trummal[a], Merle Uudsemaa[a], Meelis-Mait Sildoja[a], Juri Pahapill[a], Aleks Rebane[a,b]
[a]National Institute of Chemical Physics and Biophysics, 23 Akadeemia tee, Tallinn, Estonia 12618;
[b]Dept. of Physics, Montana State University, Bozeman, MT, USA 59715

ABSTRACT

Triamino-heptazines (TAH's) comprise the fundamental building blocks of graphitic carbon nitride, an alluring material with promising applications in optoelectronics. However, the core D_{3h} molecular symmetry enforces a forbidden lowest-energy excited singlet state, making it a challenge to characterize via conventional spectroscopy. Here, we measure one- and two-photon absorption spectra of an acidic form of triamino-heptazine, 3H-TAH, and use reversible acid/base titration to further probe the symmetry of the low-energy transitions in aqueous solution, which suggests the molecular base structure is dimelem. Two-photon absorption reveals two distinct low-energy transitions in acidic conditions, both of which are one-photon forbidden. The lowest energy state additionally becomes one-photon allowed in basic conditions. Spectroscopic changes can be described according to chromophore symmetry switching, with C_{3h}, D_{3h}, or C_s point group symmetry in respective acidic, neutral, or basic environments.

Keywords: Two-photon absorption, forbidden transition, triamino-heptazine, dimelem, symmetry switching

1. INTRODUCTION

Triamino-heptazines (TAH's) represent a class of heterocyclic compounds with a seven-membered ring structure containing alternating carbon and nitrogen atoms, decorated by amine groups. This family of compounds, starting with the monomer, melem, and extending to dimelem, melon, and eventually graphitic carbon nitride (g-C_3N_4), has attracted significant attention in materials science and chemistry due to its promising applications in catalysis, organic electronics, and solar technology.[1] Despite their structural similarity to graphene, TAH's pose a challenge for electronic and spectroscopic analysis, as inherent D_{3h} symmetry of the core structure causes the lowest excited state to be forbidden,[2] and additionally inverts the energy of the lowest singlet- and triplet excited states.[3] These attributes have made TAH a recent hot topic in both application and theoretical realms.

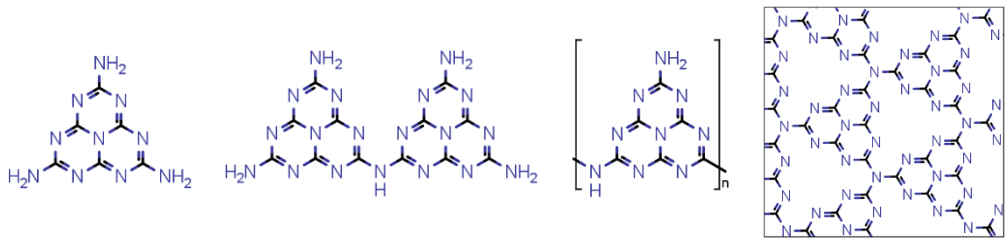

Melem Dimelem Melon g-C_3N_4

Figure 1. Structures of well-known TAH compounds: melem, dimelem, melon, and g-C_3N_4.

Two-photon absorption (2PA) spectroscopy offers an original perspective to traditional one-photon (1PA) methods, as excitations follow a unique set of selection rules.[4] Additionally, the high symmetry of the heptazine core can be lowered via acid-base chemistry,[5] providing an avenue to probe low-lying forbidden transitions via molecular symmetry-switching.[6] Here, we investigate a water-soluble TAH compound using 1PA acid/base titration and 2PA measurements. The observed spectral changes provide insights into the lowest excited states and structural symmetry of the chromophore.

*charstark@gmail.com; phone 372 5194 8502

Nonlinear Optics and its Applications 2024, edited by John M. Dudley, Anna C. Peacock, Birgit Stiller, Giovanna Tissoni, Proc. of SPIE Vol. 13004, 130040T
 · 0277-786X · doi: 10.1117/12.3022312

2. METHODOLOGY

2.1 Sample preparation, 1PA titration and model optimization

Melem was purchased from Arctom Scientific (AS040563), and placed in water that was deionized in-house. While most solid was insoluble, the supernatant could be extracted with a 0.1 μm porous filter (MiniSart, Sartorius), and this was used for all experiments. Samples were placed in a sealable 1x10 mm cuvette (21/Q/1, Starna Cells) and bubbled with argon for 10 minutes before measuring 2PA spectrum, while 1PA titration measurements were performed in a 10x10 mm cuvette (1/Q/10, Starna). Dropwise acid-base titrations were performed using either H_2SO_4 ($50\ mM$) and NaOH ($80\ mM$), with pH (Ag/AgCl, LL-Biotrode, Metrohm, calibrated via 4.01 and 7.01 buffer solutions) and 1PA spectra (UV 3600 Plus, Shimadzu) monitored at each step. The resulting absorption matrix was separated into molecular components via a multivariate curve resolution – alternating least squares (MCR-ALS) method.[6,7] Concentrations were modelled using a series of systemized reaction equilibria,[8]

$$K_{a_i} = \frac{[H][H_{i-1}M]}{[H_iM]}$$
$$C_{tot} = [H_iM] + [H_{i-1}M] + \cdots + [M] \quad (1)$$

Where K_{a_i} is the equilibrium constant between molecular species H_iM and $H_{i-1}M$, C_{tot} is the total concentration of A in the volume-corrected sample, and $[H]$ is related to the measured pH as, $[H] = 10^{-pH}$. Solving these equations for the concentration of each molecular species, $[H_iM]$, and applying initial guesses of K_a forms a list of pH dependent concentrations, $\boldsymbol{C}(pH \times i)$. These concentrations were related to the absorption matrix, $\boldsymbol{A}(pH \times \lambda)$, using the Beer-Lambert law,

$$\boldsymbol{A} = d \cdot \boldsymbol{C} \cdot \boldsymbol{\varepsilon}^T \quad (2)$$

Where d is the sample pathlength and $\boldsymbol{\varepsilon}(\lambda \times i)$ is the list of corresponding molar absorption for all molecular species. Iterative estimates of $\boldsymbol{\varepsilon}$ or $\boldsymbol{C}$ could be formed by applying the Moore-Penrose inverse of the reciprocal term ($\boldsymbol{C}^+$ or $(\boldsymbol{\varepsilon}^T)^+$) multiplied by $\boldsymbol{A}/d$. For each iteration, molar absorption spectra were modified to be non-negative, while concentrations were refit using the acid-base equilibrium description which produced updated K_a terms. This process was repeated until K_a converged, whereafter one final unconstrained MCR-ALS step was performed to estimate the goodness of fit for each pH measurement.

2.2 Two-photon excited fluorescence

Collection of 2PA spectra was performed using the two-photon excited fluorescence (2PEF) method on a previously described automated setup.[6] Breifly, <170 fs pulses were generated from a 6 kHz laser and optical parametric amplifier pair (PHAROS-SP/ORPHEUS-HE, Light Conversion), tuned to excitation wavelengths over a range, $\lambda = 545 - 845\ nm$ (FWHM bandwidth: $7 - 16\ nm$). Power dependence was controlled using a continuously variable neutral density filter wheel (NDC-100C-2, Thorlabs), monitored using a pyroelectric detector (QS-I-test, Gentec), which received a small portion of reflected beam directly before the sample. Emission spectra were collected at 90 degrees using a magic-angle polarizer followed by a monochromator (Kymera 328i, Andor) and liquid nitrogen cooled CCD (Symphony Solo, Horiba), which was integrated for up to 4 seconds to obtain the 2PEF signal, displaying a power-law dependence of 2.00 ± 0.04. Variations in the excitation pulse energy-density profile were corrected via back-to-back comparison to reference samples of Prodan, 9-chloroanthracene, 9,10-dichloroanthracene, Coumarin 153, and AF455, all of which were dissolved in toluene.[9] Quantitative 2PA measurements were not conducted due to the ultraviolet nature of 1PA excitation bands, which limited a direct quantum yield comparison; however, the relative shape of the 2PA spectrum was recorded to an estimated 5% accuracy.

3. RESULTS AND DISCUSSION

3.1 Acid/base titration and 1PA spectral decomposition

Depicted in the left of Figure 2, the TAH sample displays a structured absorption band with maxima at 283/293 nm, as well as a small shoulder near 320 nm. While titration only produces minor variation in the main absorption features, basic solutions form a new absorption band at 355 nm, displaying a notable isosbestic point at 329 nm near $4 - 9\ pH$ range. Further inspection of changes in absorption (ΔA), reveal two additional isosbestic points, shown inset, at 271 (near $9.5 - 11\ pH$) and 293.5 nm (near $2.4 - 2.6\ pH$). All spectral changes were observed to be reversible upon back titration.

Corresponding pH measurements are shown on the right of Figure 2, color coded to match with spectra on the left. Notably, the initial pH of the sample appears acidic, and when the first NaOH-equivalence point is set to 3, the second equivalence point occurs at 3.5 NaOH additions. This indicates that the TAH chromophore we observe is not melem, but is likely a protonated dimer, which we may tentatively assign as dimelem.

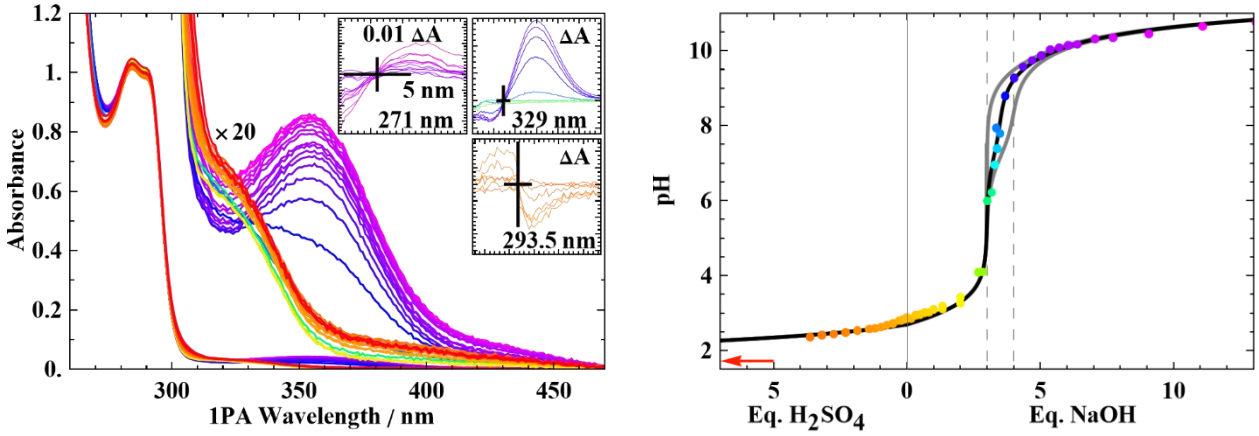

Figure 2. Dropwise titration of TAH sample with H_2SO_4 and NaOH. Left: Absorption spectra collected after each drop; insets display isosbestic points highlighted by viewing the change in absorption, $\Delta A = Base - Acid$, with black crosses for scale. Right: Corresponding pH measurements, matched to spectra via respective color; red arrow indicates the lowest pH. Gray lines highlight theoretical endpoints at 3 and 4 equivalents of NaOH, while black line provides the optimal fit of the titration model.[8]

The appearance of three unique isosbestic points indicates at least four distinct molecular species (two basic reactions, one acidic), while the clear equivalence points at 3 and 3.5 NaOH imply, respectively, protonation at three identical sites and a basic reaction for half of the TAH chromophores. Applying the MCR-ALS method (eq. 1 & 2), we find that including an additional reaction ($i = 4$) at low pH substantially improves the fit, reducing optimal residual differences between pH's predicted by the reaction model and pH's calculated by the pseudo inverse transformations. As illustrated in Figure 3, our model is discussed in terms of changes on a single TAH chromophore core, which would be doubly-linked in the case of dimelem. It comprises five molecular forms: The neutral TAH structure (green) predominates at neutral pH, reaching a maximum concentration at pH 4.8, agreeing with the reported isoelectric point of g-C_3N_4.[10] Addition of acid results in simultaneous protonation of the neutral core at three identical nitrogen sites forming 3H-TAH ($pK_a = 2.4$), conforming to known structures of triple-protonated melem.[5] Further acidification produces an additional form, labeled as 6H-TAH ($pK_a \approx 0.8$), although an isolated spectrum and quantitative analysis of structure were not resolvable due to the sparsity of data at very low pH. Addition of base proceeds in two reactive steps, the first of which may be described as an addition of hydroxide to one-half of a dimelem structure, TAH-(OH)½ ($pK_a = 7.2$). This mixed structure produces essentially a spectroscopic average of the neutral TAH chromophore and the fully hydroxylated form, TAH-OH, which forms at even higher pH ($pK_a = 9.7$), optimized as a second half-equivalent reaction. While it is known that strong bases, when heated, can replace the terminal amine groups forming cyamelurine structure[11] we do not believe this to be the case here, as the observed reaction appears reversible. We propose structures of TAH-(OH)½ and TAH-OH, with a hydroxyl-group attached out-of-plane to a carbon on the heptazine core. Such structure should be considered as only very preliminary, as optimized molecular structure calculations support it and several other structures which cannot be ignored, such as the formation of the imine anion, or attachment of hydroxyl group to one of the central carbon atoms. However, it may be safe to say that any variation effectively reduces the symmetry of the TAH chromophore to the C_s point group.

Modeled reaction equilibria appear at similar ranges to previously reported pKa's for melem[12,13] or cymeluric acid;[14,15] however, our spectral observations are extended towards the red compared to these previous investigations, and appear to display less spectral variation. This may imply that the chromophore electronic structure becomes more robust upon polymerization.

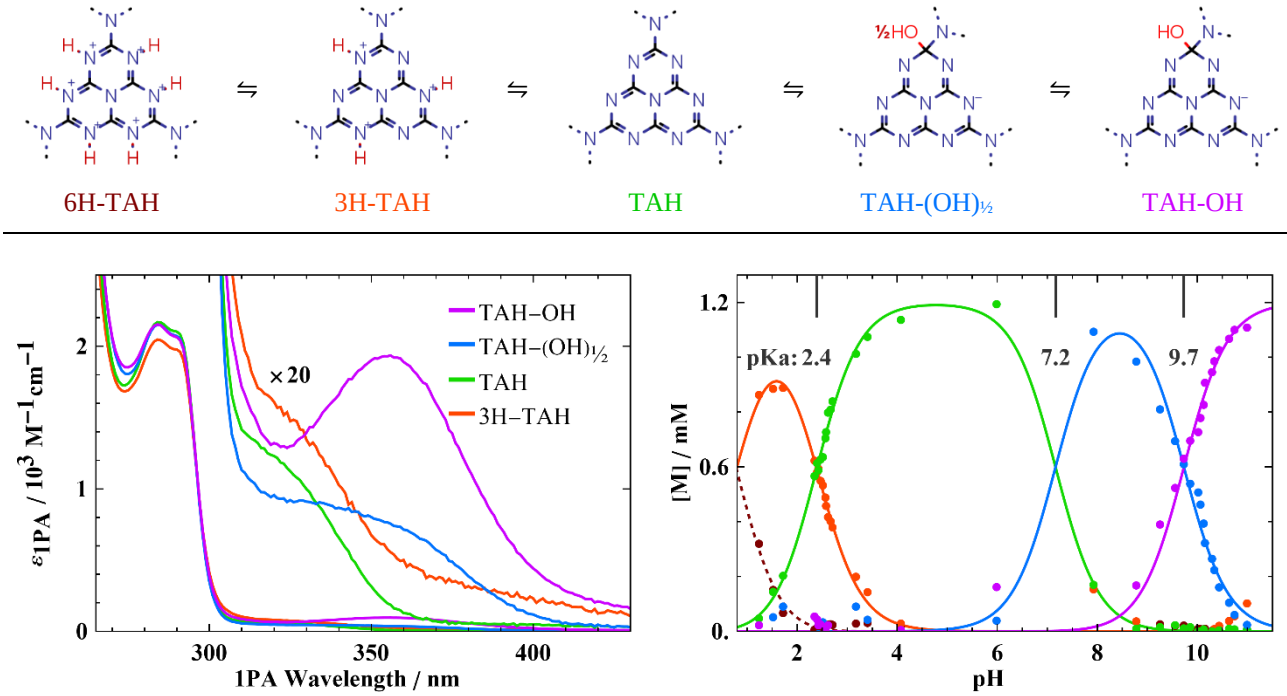

Figure 3. Five-state titration reaction model. Top: The molecular forms of the TAH chromophore. Bottom-Right: MCR-ALS optimized spectra. Bottom-Left: Corresponding pH-dependent concentrations using the model (lines), and result of a single unconstrained iteration of MCR-ALS at model convergence (points). Colors correspond to different molecular species, with an additional dark-red acidic form required to fit low-pHs, but not spectrally resolved.

3.2 Relative 2PA spectrum and comparison to 1PA

Figure 4 displays the relative 2PA spectrum of the initial TAH sample ($pH \sim 2.7$), alongside the 1PA spectra of 3H-TAH and TAH-(OH)½. The associated two-photon excited fluorescence (2PEF) spectrum, also shown in gray, displayed a single emission profile at all excitation wavelengths, implying a single dominant fluorophore. Remarkably, the acidic 2PA spectrum shows an absorption shoulder at 710 nm, closely resembling the 355 nm feature observed for 1PA under basic conditions. The 2PA spectra additionally reveals a feature at 300 nm, which does not have a corresponding 1PA band.

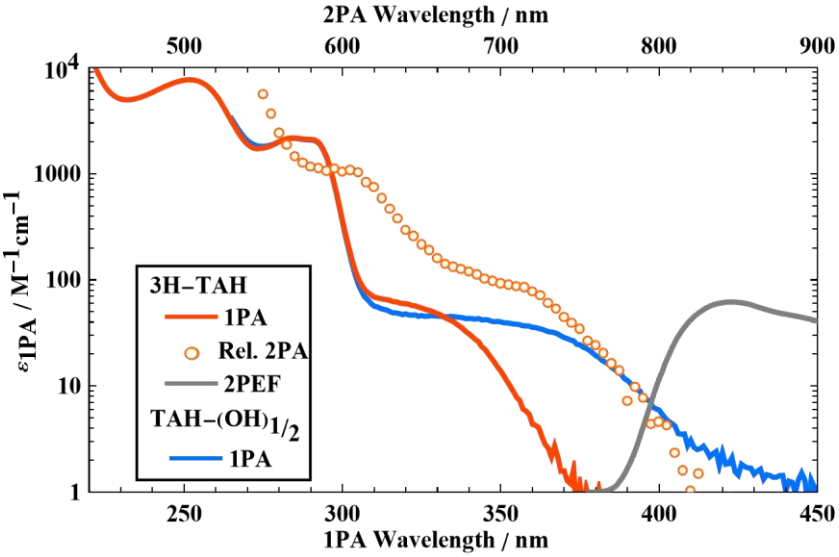

Figure 4. Comparison of acid/base 1PA spectra (colored lines) with the relative 2PA (circles) and 2PEF spectra (gray line).

Differences in appearance between 1PA and 2PA spectra often arise from the distinct selection rules governing each process.[4] Whereas 1PA spectra are dominated by transitions sharing symmetry with the linear axes, (i.e. x, y, z), two-identical-photon excitation is dictated by analogous quadratic terms, (i.e. x^2, y^2, z^2, xy, xz, yz). Furthermore, computational predictions of the lowest energy transitions, S_1 and S_2, suggest that both should be forbidden according to the natural D_{3h} symmetry.[2] The appearance of such similar lowest-energy states under different spectroscopic conditions allows us to consider symmetry switching to describe the changes in the chromophore.

Table 1 displays the D_{3h}, C_{3h} and C_s point groups associated with chromophore structures from Figure 3, and follows the 1PA and 2PA allowed transition functions according to their associated irreducible representation in each point group, with colors denoting the combined selection rules for both spectroscopies. Additionally, the two lowest-energy computationally predicted transitions are included with their associated representation. The lowest energy S_1 state, predicted to have A_2' symmetry under D_{3h} constraints, is forbidden for the neutral TAH structure, but becomes 2PA allowed when switching to the propeller-like 3H-TAH, and is both 1PA and 2PA allowed when symmetry is reduced to mirror-plane structures under basic conditions, matching our experimental observations. Furthermore, the predicted energy of this state for dimelem matches the observed shoulder, providing additional support for this molecular structure.

Table 1. Point group symmetries for different forms of TAH, with associated irreducible representations of observable and calculated transitions. Transitions are colored according to allowedness in either 1PA (Blue), 2PA (Red), both 1PA and 2PA (Green), or forbidden for both (Gray).

Function[a]	6H-TAH TAH D_{3h}	3H-TAH C_{3h}	TAH-(OH)½ TAH-OH C_s	λ_{1PA}, nm
x^2+y^2, z^2	A_1'	A'	A'	355
S_1[b]	A_2'	A'	A'	356[b]
S_2[b]	A_1''	A''	A''	-
z	A_2''	A''	A'	320
(xz, yz)	E''	E''	A' A''	300
(x, y) (x^2-y^2, xy)	E'	E'	A' A''	283/293

[a]Axes orientation determined from the D_{3h} symmetry group. [b]Excited state symmetries and energy for S_1 and S_2 taken from [2].

A similar condition is expected for S_2 excitation, being forbidden for the neutral TAH chromophore, but 1PA allowed in all reduced-symmetry forms. While we do observe a minor 1PA shoulder near 320 nm, this shoulder appears also in the neutral spectrum (Figure 3, Green) suggesting that in this case symmetry switching does not match expectations for the single TAH chromophore. This may be an indication that this higher-energy transition involves two TAH centers, or that symmetry breaking is more notable in this case. This concept may be extended to the large 2PA feature at 300 nm, which is not observed in 1PA at any point, although according to an expected E'' symmetry this should become 1PA allowed in basic solution. Perhaps basic environments disrupt higher-energy transitions more than the lowest excited state.

4. CONCLUSIONS

In summary, we have investigated a water-soluble triamino-heptazine compound, which we tentatively assign as a protonated form of dimelem. In strongly basic solutions, we reveal a low-energy transition using one-photon absorption spectroscopy, which appears to closely match the two-photon absorption under acidic conditions. We construct a model of acid/base equilibria and compare the resulting symmetry switching behavior to observations in this low-energy band. While this model accurately describes the lowest energy state, matching with computational predictions for dimelem, higher-lying transitions appear to have more complex behavior, requiring further investigation.

ACKNOWLEDGEMENTS

This work was supported by the Ministry of Education and Research, Republic of Estonia (grants PRG661 and PSG317). A. Rebane acknowledges support from the NSF Award 210362. We thank Heiki Vija for the use of the pH probe.

REFERENCES

[1] Savateev, O., Antonietti, M. and Wang, X., eds., [Carbon Nitrides: Structure, Properties and Applications in Science and Technology], De Gruyter (2023).

[2] Ehrmaier, J., Rabe, E. J., Pristash, S. R., Corp, K. L., Schlenker, C. W., Sobolewski, A. L. and Domcke, W., "Singlet–Triplet Inversion in Heptazine and in Polymeric Carbon Nitrides," J. Phys. Chem. A **123**(38), 8099–8108 (2019).

[3] Aizawa, N., Pu, Y.-J., Harabuchi, Y., Nihonyanagi, A., Ibuka, R., Inuzuka, H., Dhara, B., Koyama, Y., Nakayama, K., Maeda, S., Araoka, F. and Miyajima, D., "Delayed fluorescence from inverted singlet and triplet excited states," Nature **609**(7927), 502–506 (2022).

[4] McClain, W. M., "Excited state symmetry assignment through polarized two-photon absorption studies of fluids," J. Chem. Phys. **55**(6), 2789–2796 (1971).

[5] Sattler, A. and Schnick, W., "Melemium Hydrogensulfate $H_3C_6N_7(NH_2)_3(HSO_4)_3$ – the First Triple Protonation of Melem," Z. Für Anorg. Allg. Chem. **636**(15), 2589–2594 (2010).

[6] Stark, C. W., Rammo, M., Trummal, A., Uudsemaa, M., Pahapill, J., Sildoja, M.-M., Tshepelevitsh, S., Leito, I., Young, D. C., Szymański, B., Vakuliuk, O., Gryko, D. T. and Rebane, A., "On-off-on control of molecular inversion symmetry via multi-stage protonation: Elucidating vibronic Laporte rule," Angew. Chem. Int. Ed., e202212581 (2022).

[7] de Juan, A., Jaumot, J. and Tauler, R., "Multivariate Curve Resolution (MCR). Solving the mixture analysis problem," Anal. Methods **6**(14), 4964–4976 (2014).

[8] Morales, D. A., "Mathematical modeling of titration curves," J. Chemom. **16**(5), 247–260 (2002).

[9] Rebane, A., "2PADB," Two-Photon Absorpt. 2PA Spectra Database, 2019, <https://kbfi.ee/mpa/>.

[10] Zhu, B., Xia, P., Ho, W. and Yu, J., "Isoelectric point and adsorption activity of porous g-C_3N_4," Appl. Surf. Sci. **344**, 188–195 (2015).

[11] Horvath-Bordon, E., Kroke, E., Svoboda, I., Fueß, H., Riedel, R., Neeraj, S. and Cheetham, A. K., "Alkalicyamelurates, $M_3[C_6N_7O_3]\cdot xH_2O$, M = Li, Na, K, Rb, Cs: UV-luminescent and thermally very stable ionic tri-s-triazine derivatives," Dalton Trans(22), 3900–3908 (2004).

[12] Finkel'shtein, A. I. and Spiridonova, N. V., "Chemical properties and molecular structure of derivatives of sym-heptazine[1,3,4,6,7,9,9b-heptaazaphenalene, tri-1,3,5-triazine]," Russ. Chem. Rev. **33**(7), 400–405 (1964).

[13] Takimoto, M., "Studies on ultraviolet absorption spectra and structures of simple cyanamide derivatives," Chem. Soc. Jpn. **85**, 159–168 (1964).

[14] Redemann, C. E. and Lucas, H. J., "Ionization Constants and Hydrolytic Degradations of Cyameluric and Hydromelonic Acids," J. Am. Chem. Soc. **61**(12), 3420–3425 (1939).

[15] El-Gamel, N. E. A., Seyfarth, L., Wagler, J., Ehrenberg, H., Schwarz, M., Senker, J. and Kroke, E., "The tautomeric forms of cyameluric acid derivatives," Chem. - Eur. J. **13**, 1158–1173 (2007).